(第3号様式)(Form No. 3)

学 位 論 文 要 旨
Dissertation Summary

氏　　名 (Name) 藤 良太郎

論　文　名：
(Dissertation Title) Tsunami detection method using high-frequency ocean surface radar
海洋短波レーダを用いた津波検知技術

Mitigating disasters caused by huge tsunamis is a particularly crucial issue in Japan. High-frequency ocean surface radar (HF radar) provides the great advantage of observing a wide range of ocean surface currents. It is counted on to be applied to tsunami mitigation and yet few studies have been conducted. This research aims to examine tsunami detection performance of HF radar by using a novel technique—a virtual tsunami observation experiment—and to establish a real-time tsunami detection technique.

Regarding tsunami detection, the combination of HF radar and a tsunami detection method should be assessed as the onshore-offshore distribution of tsunami detection probability, because the probability will vary in accordance with the signal-to-noise ratio (SNR) and the tsunami magnitude in addition to the radar system specifications. However, no previous studies have discussed the distance and the earliness statistically based on a number of tsunami observations. This is because actual tsunami detection using HF radars is limited to the 2011 Japan and the 2012 Indonesian tsunamis except for some meteotsunami observations (e.g., Lipa et al. 2014). Considering the low probability of tsunami occurrence, it is unlikely to be possible to obtain many more tsunami observations in the near future.

Three minutes after the 2011 Tohoku-Oki earthquake, the first warning, which underestimated the tsunami height (sea surface displacement induced by the tsunami), was issued by the Japan Meteorological Agency (JMA). The category of warning was revised upward 28 min after the earthquake (Ozaki 2011) by the JMA based on the tsunami heights—measured by a GPS wave gauge (NOWPHAS: Nationwide Ocean Wave Information Network for Ports and Harbours, http://www.mlit.go.jp/kowan/nowphas/index_eng.html) installed off the Tohoku coast. The underestimation, which eventually led to greater damage

(e.g., Takahashi and Konuma 2011; Seto and Takahashi 2015), was caused by saturation of the magnitude calculated by seismometer measurements. No other tsunami warning system is in operation except that of the JMA in Japan. The underestimation of a tsunami warning is a major concern for the huge tsunamis with a maximum tsunami height exceeding 30 m generated by Nankai Trough earthquakes. Therefore, in addition to detecting the tsunami arrival offshore, it is crucial to estimate tsunami heights and check the category of tsunami warning issued by the JMA by using measured tsunami heights or tsunami-induced velocities in order to mitigate and understand tsunami impacts in coastal regions. Moreover, to examine earliness of the tsunami detection is also crucial since the tsunamis induced by Nankai Trough earthquakes are expected to reach the coast within a few minutes.

Hence, we statistically examined the tsunami detection distance and earliness of the detection based on virtual tsunami observation experiments by using signals received in February 2014 by HF radar installed on the southern coast of Japan and numerically simulated velocities induced by a Nankai Trough earthquake. In the experiments, the Doppler frequencies associated with the simulated velocities were superimposed on the receiving signals of the radar, and the radial velocities were calculated from the synthesized signals by the fast Fourier transform. Tsunami was then detected based on the temporal change in the cross-correlation of the velocities, before and after tsunami arrival, between two points 3 km apart along a radar beam.

First, we performed virtual tsunami observation experiments through a "*posteriori analysis*" using received signals of the NJRC radar installed on the Mihama coast and a Nankai Trough tsunami simulation based on the fault model case 3 in order to overcome the difficulty of obtaining more tsunami observations and to statistically examine the detection distance and quantitatively examine the nearshore tsunami heights inferred from offshore velocities. In these experiments, Doppler frequencies associated with the tsunami-induced current velocities simulated by a numerical model were superimposed on the receiving signals actually observed during February 2014 by using the method proposed by Gurgel et al. (2011). The synthesized signals were analyzed and radial velocities were calculated by the fast Fourier transform (FFT). The tsunami was then detected by using a method similar to that in Fuji et al. 2015. We then assessed the combination of the NJRC radar system and the detection method mainly by using detection probability with respect to the offshore distance from the radar. Also, we quantitatively examined the measured tsunami-induced velocities (i) by comparing the tsunami warning categories inferred from the numerical simulation and from the offshore velocity measurements by the radar, and (ii) by estimating the degree of coincidence of the observed- and simulated velocity variability using variance reduction.

From the experiment, we found that the possibility of tsunami detection primarily depends on the kinetic energy ratio between tsunami and shorter-period BGC velocities. In the onshore-offshore direction, the monthly average detection probability is over 90% when the energy ratio exceeds 5 (offshore distance: 9 km $\leq L \leq$ 36 km and water depth: 50 m $< h <$ 600 m) and is about 50% when the energy ratio is approximately 1 (L = 42 km, h = 1200 m) (Fig. 1). For a certain range cell on the radar beam, the energy ratio temporally varied in accordance with the variations of ocean surface wave height, ionospheric electron density and also with the shorter-period BGC physics. The

results—namely that the tsunami detection distance strongly depends on the energy ratio between tsunami and shorter-period BGC velocities, and sea surface state as well as receiving noise—are the most important and general findings of the experiments. These demonstrate that the virtual tsunami observation experiments for other seasons and/or for other coastal regions are required to comprehensively understand the tsunami detection performance of high-frequency radars.

Second, we performed virtual tsunami observation experiments through a "*real-time analysis*". Then assessed earliness of detection of tsunami wavefront. The detection results were compared with previous method using q-factor proposed by Lipa et al. (2012a, b, 2014) and the applicability of the method was discussed. We found that the possibility of tsunami wave front detection primarily depends on the kinetic energy ratio even in real-time detection. However, the energy ratio required for tsunami wavefront detection is one order of magnitude less than that by "posteriori analysis". The maximum detection distance with 80% detection probability and 4-min time lag was 22.5 km (corresponding energy ratio is of the order of 10^0). Tsunami arrival was detected approximately within 3–5 min after the time of manifestation of tsunami-induced velocity in ranges from 3 to 22.5 km with 80% detection probability. The developed technique is superior in terms of its ability to detect subsequent tsunami waves in addition to tsunami wavefront—with no misdetection (Fig. 2).

The proposed method in this study using cross-correlation is also outstanding in terms of its ability to detect tsunami in a quantitative manner, which enables it to mitigate tsunami impact—such as to check the category of tsunami warning issued by the JMA, estimate tsunami height along the coast, and estimate tsunami source based on the inversion method which allows it to specify devastating damaged areas by numerical simulation—in addition to tsunami detection. HF radar can widely observe ocean surface currents. We examined the tsunami detection performance focusing on beam 04 in this study, but the present method can be easily applied to the whole observed area.

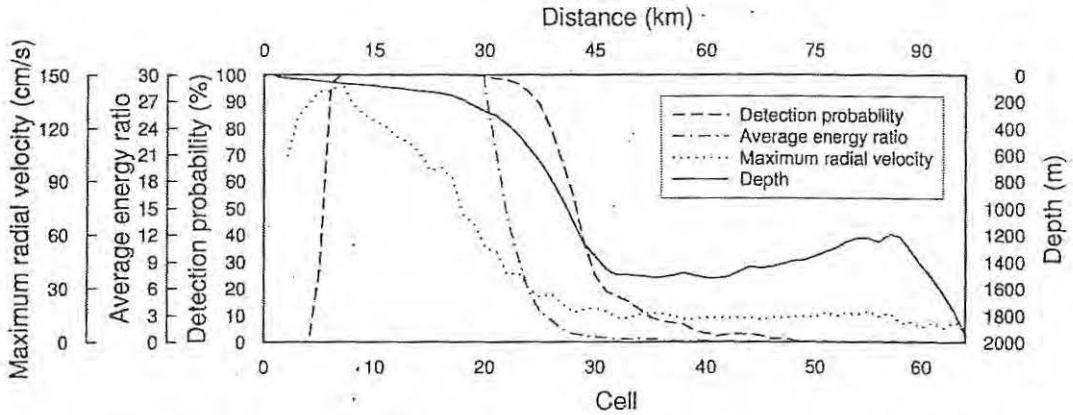

Fig. 1 Onshore-offshore distributions of the tsunami detection probability in February 2014 (*dashed blue*), the monthly average energy ratio (*dashed-dotted green*), the maximum tsunami-induced radial velocity (*dotted red*), and the water depth (*solid black*) along beam 04.

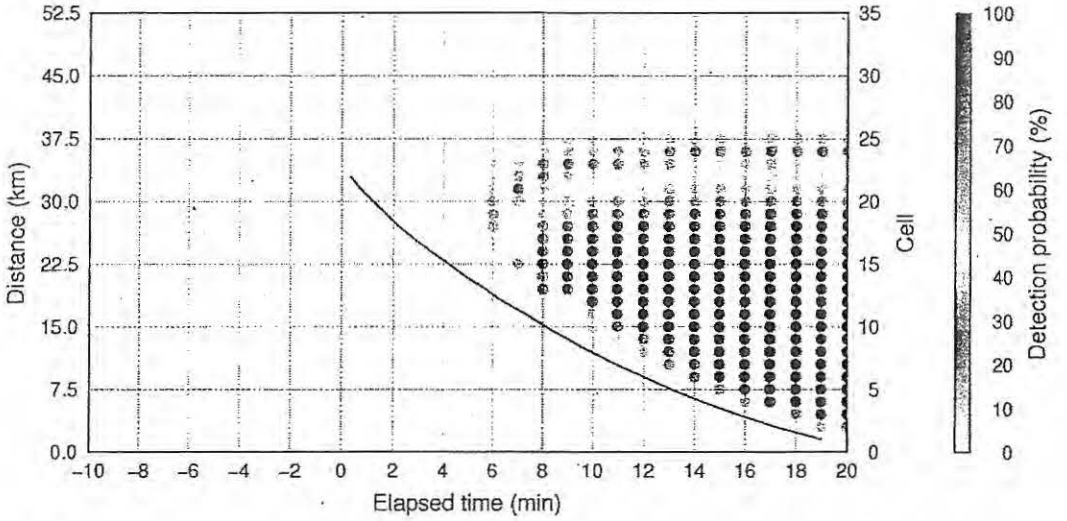

Fig. 2 Time-distance plot of real-time detection probability of February 2014. The *pink line* (theoretical tsunami wavefront) represents theoretical curve calculating back propagation with a speed of linear long-wave started from the time of tsunami arrival at the coast.